# SIMULATION OF A TURBULENT FLOW IN A ROTATING PIPE USING THE STRUCTURE-BASED MODEL

**Svetlana V. Poroseva[*], Stavros C. Kassinos, Carlos A. Langer, William C. Reynolds**
Center for Turbulence Research
Department of Mechanical Engineering, Stanford University
Stanford, CA 94305, USA
poroseva@ctr.stanford.edu

## ABSTRACT

In the present work, the structure-based model (SBM) was evaluated in a turbulent flow in a cylindrical pipe rotating around its longitudinal axis. It was found that the SBM is able to predict the flow accurately at various Reynolds numbers and under stronger rotation than what is possible with the Reynolds stress transport models (RSTMs). In a fully developed pipe flow, the SBM, being a linear model, slightly improves the profiles obtained with the non-linear RSTM (Speziale et al., 2000). However, like the RSTMs do, the SBM significantly overpredicts the turbulent kinetic energy level in this part of flow in comparison with the results of experiments.

## INTRODUCTION

Mean rotation induces dynamical effects on turbulence that enter transport equations through the non-local pressure-containing correlation. It was shown in Reynolds & Kassinos (1995) and later in Kassinos et al. (2001) that to describe this effect accurately in inhomogeneous turbulence, a one-point turbulence closure should include a minimal set of independent tensors that carry information not contained in the Reynolds stresses $R_{ij}$. This set of tensors include, in addition to $R_{ij}$, two second-rank tensors: *dimensionality* $D_{ij}$ and *circulicity* $F_{ij}$, as well as the third-rank *stropholysis* tensor $Q^*_{ijk}$. Relying on these ideas, the SBM has been developed (Reynolds & Kassinos, 1995; Kassinos & Reynolds, 1997) and tested successfully for a wide range of deformations of homogeneous turbulence as well as for some simple wall-bounded flows (Kassinos et al., 2000).

Currently, the SBM is being used for the computation of complex inhomogeneous turbulent flows with imposed system rotation. Here we report on the case of a turbulent flow in an axially rotating pipe. Despite the simple geometry, the structure of turbulence in a rotating pipe flow changes substantially both as the flow develops with downstream distance from the pipe entrance and with increasing rotation rate, and as a result this flow serves as a severe benchmark for any turbulence closure. From a practical point of view, the modeling of a turbulent pipe flow is of interest because it relates to phenomena encountered in various engineering systems involving boundary layers on rotating surfaces, *e.g.*, heat exchangers and rotor cooling systems.

## MODEL OUTLINE

Information carried by the turbulence structure tensors and the Reynolds stresses can be obtained from a single third-rank tensor $\mathbf{Q}$ (Reynolds & Kassinos, 1995), which relates to the other tensors as:

$$D_{ij} = \epsilon_{imp} Q_{pmj}, \quad F_{ij} = \epsilon_{imp} Q_{jpm}$$

$$R_{ij} = < u_i u_j > = \epsilon_{imp} Q_{mjp}, \quad Q^*_{ijk} =$$

$$\frac{1}{6}\left[Q_{ijk} + Q_{jki} + Q_{kij} + Q_{ikj} + Q_{jik} + Q_{kji}\right] \quad (1)$$

Therefore, the SBM considered in this work, includes a model transport equation for the one-point tensor $\mathbf{Q}$, which in an inhomogeneous flow takes the form (Kassinos et al., 2000):

$$\frac{DQ_{ijk}}{Dt} = \left[\left(\nu\delta_{mn} + \frac{C_\nu}{\sigma_Q} T R_{mn}\right) Q_{ijk,m}\right]_{,n} + k f_{ijk} + H_{ijk} \quad (2)$$

where $H_{ijk} = -G_{jm} Q_{imk} - \frac{1}{2} G_{tm} \epsilon_{tik} R_{mj} + \frac{1}{2}(Q_{imk} + Q_{kmi}) - \frac{1}{T} Q_{ijk}$

[*] also affiliated with the Institute of Theoretical and Applied Mechanics, SD RAS, 630090 Novosibirsk, RUSSIA

Here, $G_{ij} = U_{i,j}$, $2k = q^2 = R_{ii}$, $\varepsilon$ is the dissipation rate, $\delta_{ij}$ is the Kronecker delta tensor, $\epsilon_{ijk}$ is the Levi-Civita alternating tensor, $\nu$ is the kinematic viscosity. Time scale $T$ is modeled as $T = \sqrt{(k/\varepsilon)^2 + 36 \cdot \nu/\varepsilon}$ (Durbin, 1993). Model coefficients are: $C_\nu = 0.22$ and $\sigma_Q = 1$.

Near-wall effects are incorporated in (2) through an elliptic relaxation tensorial function $f_{ijk}$. This function models redistributive processes in inhomogeneous turbulence and its components are found from an equation

$$L^2 \nabla^2 f_{ijk} - f_{ijk} = -\frac{\Pi_{ijk}}{k} \qquad (3)$$

similar to the one suggested in Durbin (1993). $\Pi_{ijk}$ describes redistributive processes in homogeneous turbulence. The model for $\Pi_{ijk}$ is discussed in detail in Kassinos et al. (2000).

For the length scale $L$, various functional forms have been tested. However, the best results were obtained using a simple function like $L^+ = 1$, at $y^+ \leq 60$, and $L^+ = 0$, at $y^+ \geq 60$. It is worth noting that in the initial section of the rotating pipe, where strong suppression of turbulence statistics occurs, the influence of this length scale is rather weak. At a rotation number of $N = 0.6$ both the peak value and the extent of the profile of $L$ from the pipe wall seem to have practically no influence on the results of the calculations. The rotation number $N$ is defined as the ratio of the pipe wall velocity $W_o$ to the mean flow velocity at the pipe center $U_o$.

Because the main goal of the present work was to compare the performance of the $Q_{ijk}$-equation with that of the $R_{ij}$-equation in a complex rotated turbulent flow, the standard equation for the dissipation rate

$$\frac{D\varepsilon}{Dt} = \left[\left(\nu\delta_{jk} + \frac{C_\nu}{\sigma_\varepsilon} T R_{jk}\right)\varepsilon_{,j}\right]_{,k} - \frac{1}{T}\left(C_o\varepsilon - C_s P\right) \qquad (4)$$

was used as the basic one. Here, $P = -R_{ij}U_{i,j}$. Model coefficients are: $C_o = 11/6$, $\sigma_\varepsilon = 1.1$. To describe a flow at different Reynolds numbers, the coefficient $C_s$ has to vary from 1.58 at $Re_o = 4 \cdot 10^4$ to 1.65 at $Re_o = 7 \cdot 10^3$. In both cases this value differs from the value found optimal for a homogeneous flow, that is, $C_s = 1.5$. The similar situation is observed when the RSTMs are used.

An alternative to equation (4) was also tested. It was shown in Kurbatskii et al. (1995), that if one assumes the model coefficient $C_o$ to be a function of the Richardson number

$$C_o^* = \max(1.4, C_o(1 - C_R Ri)), \quad C_R = 2$$

$$Ri = \frac{\frac{\partial W}{\partial r} \cdot \frac{W}{r}}{\left(\frac{\partial W}{\partial r}\right)^2 + \left(\frac{\partial U}{\partial r}\right)^2}$$

the effects of moderate rotation on a flow in an initial pipe section can be successfully reproduced. Here, $U$ and $W$ are the axial and the angular mean velocity components respectively, $r$ is the radial coordinate. The restrictive condition on the value of $C_o^*$ is imposed to avoid excessive values of the dissipation rate close to a wall, which can occur under rotation.

The modification of $C_o$ proposed by Kurbatskii et al. (1995) is applied in the present work

$$\frac{D\varepsilon}{Dt} = \left[\left(\nu\delta_{jk} + \frac{C_\nu}{\sigma_\varepsilon} T R_{jk}\right)\varepsilon_{,j}\right]_{,k} - \frac{1}{T}\left(C_o^*\varepsilon - C_s P\right) \qquad (5)$$

Thus, two sets of model equations: (2)–(4) and (2), (3), (5), with the standard transport equations for the mean velocity components form two models: Q1 and Q2, investigated in this work.

## NUMERICAL PROCEDURE

To compute a pipe flow, all equations were written using the boundary layer approximation in the axisymmetric cylindrical frame of reference $x^i = (x, r, \varphi)$, where $x$, $r$, and $\varphi$ are axial, radial, and angular coordinates respectively. The control volume technique was used to solve transport equations. Equation (3) was solved using a standard finite-difference scheme. The grid was non-uniform in $r$, with the total number of nodes being 64 for $Re_o = U_o D/\nu = 4 \cdot 10^4$ and 81 for $Re_o = 7 \cdot 10^3$ ($D$ is the pipe diameter, $R = D/2$).

In the computation we used the same conditions as those in the experiments (*e.g.*, Kikuyama et al., 1983; Zaets et al., 1985), where a swirling flow was obtained by conveying a fully-developed turbulent flow from a stationary cylindrical pipe into a rotating cylindrical section of the same diameter.

On the pipe axis the boundary conditions are:

$$\frac{\partial U}{\partial r} = \frac{\partial \varepsilon}{\partial r} = W = 0, \quad U = U_o$$

$$\frac{\partial Q_{ijk}}{\partial r} = 0, \quad \text{if } i \neq j \neq k$$

$$Q_{ijk} = 0, \quad \text{if } i = j, \text{ or } j = k, \text{ or } i = k$$

At the wall,

$$U = Q_{ijk} = 0, \quad W = W_o, \quad \varepsilon_w = \frac{2\nu k_w}{y_w^2}$$

where $k_w$ is the value of the turbulent kinetic energy at the last grid node next to the wall and $y_w$ is the distance between the wall and that node. This last condition ensures that $k_w = O(y_w^2)$.

Near a pipe wall, the behavior of $Q_{ijk}$-components should be consistent with the correct behavior of the corresponding Reynolds stresses in accordance with (1). Such behavior of $Q_{ijk}$ was obtained with applying appropriate boundary conditions on $f_{ijk}$:

$$f^{(w)}_{\alpha\beta\gamma} = -\frac{20\nu^2 Q_{\alpha\beta\gamma}}{\varepsilon_w y_w^4}, \quad \text{where}$$

$(\alpha\beta\gamma)$=$(xx\varphi)$, $(\varphi\varphi x)$, $(x\varphi\varphi)$, $(\varphi xx)$, $(\varphi rx)$,$(xr\varphi)$

$$f^{(w)}_{xx\varphi} = -f^{(w)}_{rr\varphi}, \quad f^{(w)}_{\varphi\varphi x} = -f^{(w)}_{rrx}$$

$$f^{(w)}_{x\varphi\varphi} = -f^{(w)}_{xrr}, \quad f^{(w)}_{\varphi xx} = -f^{(w)}_{\varphi rr}$$

$$f^{(w)}_{r\varphi x} = -0.2 f^{(w)}_{xr\varphi}, \quad f^{(w)}_{\varphi xr} = -0.8 f^{(w)}_{xr\varphi}$$

$$f^{(w)}_{x\varphi r} = -0.2 f^{(w)}_{\varphi rx}, \quad f^{(w)}_{rx\varphi} = -0.8 f^{(w)}_{\varphi rx}$$

The rest of the components are equal to zero at the wall. On the pipe axis, the boundary conditions for $f_{ijk}$ are the same as for $Q_{ijk}$.

## RESULTS AND DISCUSSION

### Stationary pipe

Without rotation, both models: Q1 and Q2, coincide. Calculations have been done at two Reynolds numbers: $Re_o = 7 \cdot 10^3$ and $Re_o = 4 \cdot 10^4$, to verify the ability of the Q-model to give reasonable results in both low and high Reynolds number regimes. As shown in Figures 1 and 2, the model gives quite good results.

For comparison, profiles obtained with the linear (IP) RSTM (Kurbatskii et al., 1995) are also presented. Though this model reproduces turbulent characteristics and mean velocity well at the high Reynolds number, it describes only qualitatively the features of the low Reynolds number flow.

As experiments demonstrate (*e.g.*, Kikuyama et al., 1983; Zaets et al., 1985), it is possible to distinguish two regions in a rotating pipe flow with different turbulence structure. In the initial section of a pipe with length of about $30D$, strong suppression of turbulence characteristics is observed. After suppression, however, they increase in value and eventually stabilize on a high level. This is the region of fully developed turbulence, which is observed at about $170D$ for any $Re$.

### Initial section of a rotating pipe

Calculations have been done at $Re_o = 4{\cdot}10^4$. Figures 3,4,6 correspond to the pipe section $x/D = 25$. For comparison, profiles obtained with the RSTMs: IP and non-linear (SSG) (Speziale et al., 2000), also are given. In both RSTMs, damping functions (Gibson & Launder, 1978) were applied to describe wall effects.

It was found that to reproduce correctly the effect of strong turbulence suppression in this region, the Q-model as well as the IP and the SSG models should include modified $\varepsilon$-equation (5). We denote such non-linear model as SSG1.

The Q-model describes quite well the axial velocity profile in the whole flow area: from the wall to the pipe axis at different rotation numbers (Fig. 3). Moreover, the Q-model computes correctly the dynamics of the axial velocity with increasing rotation. That is, at the low rotation number $N = 0.15$, the axis value of $U$ slightly decreases, but with further increase of $N$, it begins to grow. The behavior of the angular component of the mean flow velocity also is reproduced well. Turbulent statistics are described very well, especially near the pipe axis (Figs. 4,6). This is an important result, because turbulent transport at the core of a pipe flow at moderate swirl is similar to turbulent transport in concentrated vortex formations in the atmosphere.

Note that in the initial pipe section, the performance of two RSTMs are comparable with each other.

### Fully developed flow

With increasing rotation and distance from the pipe entrance, the Q2-model as well as the IP and the SSG1 models predict full suppression of the turbulence in contradiction with experimental data. A fully developed turbulent flow in a rotating pipe was computed with the Q1-model. The results are compared (Fig. 7) with the data obtained with the SSG model in which equation (4) is used to describe dissipative processes and near-wall effects are taken into account through the elliptic relaxation scheme (Durbin, 1993). We denote this model as SSG2.

The model reproduces better than the

RSTMs the evolution of the axial component of the mean velocity. For the angular velocity, the computational results obtained with the Q1-model are close to the profiles obtained with the linear RSTMs (Pettersson et al., 1998; Speziale et al., 2000; Kurbatskii & Poroseva, 1999). The SSG2 model provides better agreement for $W$ with experimental data. The shear stresses are reproduced well by the Q1-model. However, in this part of the flow, like the RSTMs do, the Q1-model significantly overpredicts the turbulent kinetic energy level in comparison with experimental data.

Most importantly, the Q-model is able to reproduce the correct behavior of turbulence characteristics at relatively high rotation rates, *e.g.*, $N = 1$, whereas the RSTMs predict relaminarization of the flow (Pettersson et al., 1998) at this $N$ in contrast to the experiments (Kikuyama et al., 1983), which show no sign of turbulence disappearance even at considerably higher $N$.

## CONCLUSIONS

The Q-model is able to predict the flow accurately at various Reynolds numbers. In a fully developed pipe flow at moderate rotation numbers, the Q-model, being linear, slightly improves the profiles obtained with the non-linear RSTM, which gives the best results among the RSTMs for this part of flow (Pettersson et al., 1998). Most importantly, the Q-model is able to reproduce the correct behavior of turbulence characteristics at relatively high rotation rates, *e.g.*, $N = 1$, whereas the RSTMs predict relaminarization of the flow in contrast to experiments. Also, under some parameter combinations ($N$, $Re$) computations using the RSTMs fail to converge (Pettersson et al., 1998; Kurbatskii & Poroseva, 1999), whereas such difficulties have not been encountered with the Q-model.

However, the Q-model as tested in this work, does not solve all problems. One of the possible reasons for this, is that in order to be consistent, a one-point turbulence closure based on the transport equation for $\mathbf{Q}$ should also include structure information in the equation for the dissipation rate $\varepsilon$. We are currently working in this direction. In the RSTMs, such modifications would not be possible since they do not carry the necessary information.

## REFERENCES


Durbin, P., 1993, "A Reynolds-stress model for near-wall turbulence", *J. Fluid Mech.*, Vol.249, pp. 465–498.

Eggels, J. G. M. et al., 1994, "Fully developed turbulent pipe flow: a comparison between direct numerical simulation and experiment", *J. Fluid Mech.*, Vol.268, pp. 175–209.

Gibson, M. M., and Launder, B. E., 1978, "Ground effects on pressure fluctuations in the atmospheric boundary layer", *J. Fluid Mech.*, Vol.86, pp. 491–511.

Imao, S. et al., 1996, "Turbulent characteristics of the flow in an axially rotating pipe", *Int.J. Heat Fluid Flow*, Vol.17(5), pp. 444–451.

Kassinos, S. C., and Reynolds, W. C., 1997, "Advances in structure-based modeling", Annual Research Briefs, Center for Turbulence Research, NASA Ames/Stanford University, pp. 179–193.

Kassinos, S. C. et al., 2000, "Structure-based turbulence modeling for wall-bounded flows", *Int.J. Heat Fluid Flow*, Vol.21, pp. 599–605.

Kassinos, S. C. et al., 2001, "One-point turbulence structure tensors", *J. Fluid Mech.*, Vol.428, pp. 213–248.

Kikuyama, K. et al., 1983, "Flow in an axially rotating pipe (a calculation of flow in the saturated region)", *Bull. JSME*, Vol.26(214), pp. 506–513.

Kurbatskii, A. F. et al., 1995, "Calculation of statistical characteristics of a turbulent flow in a rotated cylindrical pipe", *High Temperature*, Vol.133(5), pp. 738–748.

Kurbatskii, A. F., and Poroseva, S. V., 1999, "Modelling turbulent diffusion in a rotating cylindrical pipe flow", *Int.J. Heat Fluid Flow*, Vol.20(3), pp. 341–348.

Pettersson, B. A. et al., 1998, "Modeling near-wall effects in axially rotating pipe flow by elliptic relaxation", *AIAA Journal*, Vol.36(7), pp. 1164–1170.

Reynolds, W. C., and Kassinos, S. C., 1995, "A one-point model for the evolution of the Reynolds stress and structure tensors in rapidly deformed homogeneous turbulence", *Proc. Roy. Soc. London A*, Vol.451(1941), pp. 87–104.

Speziale, C.G. et al., 2000, "Analysis and modeling of turbulent flow in an axially rotating pipe", *J. Fluid Mech.*, Vol.407, pp. 1–26.

Zaets, P. G. et al., 1985, "Experimental study of the behavior of turbulence characteristics in a pipe rotating around its axis (in Russian)," *Modern problems of continuous medium mechanics*, Moscow Physics and Technics Inst., pp. 136–142.

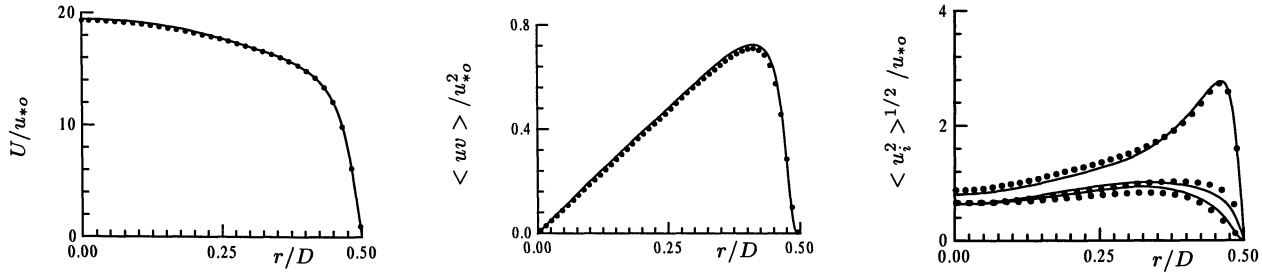


Figure 1: Stationary pipe flow ($Re_o = 7 \cdot 10^3$): (—— ) Q–model, (•) DNS data (Eggels et al., 1994)

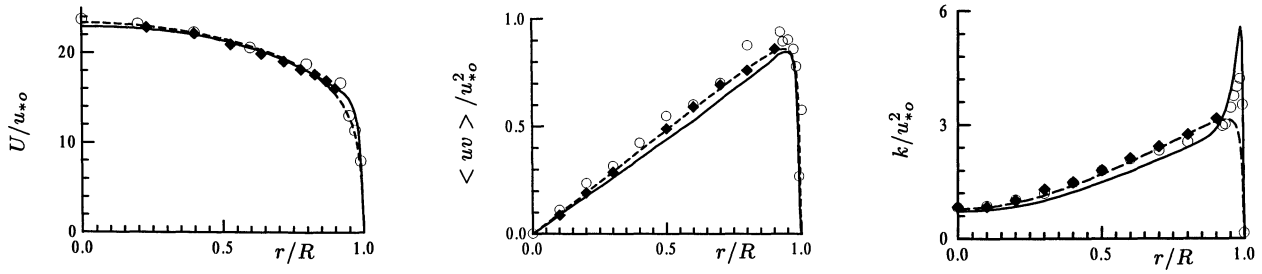


Figure 2: Calculations ($Re_o = 4 \cdot 10^4$): ( —— ) Q, (--- ) IP;
experiments: (♦) Zaets et al. (1985), (o) Laufer (1954)

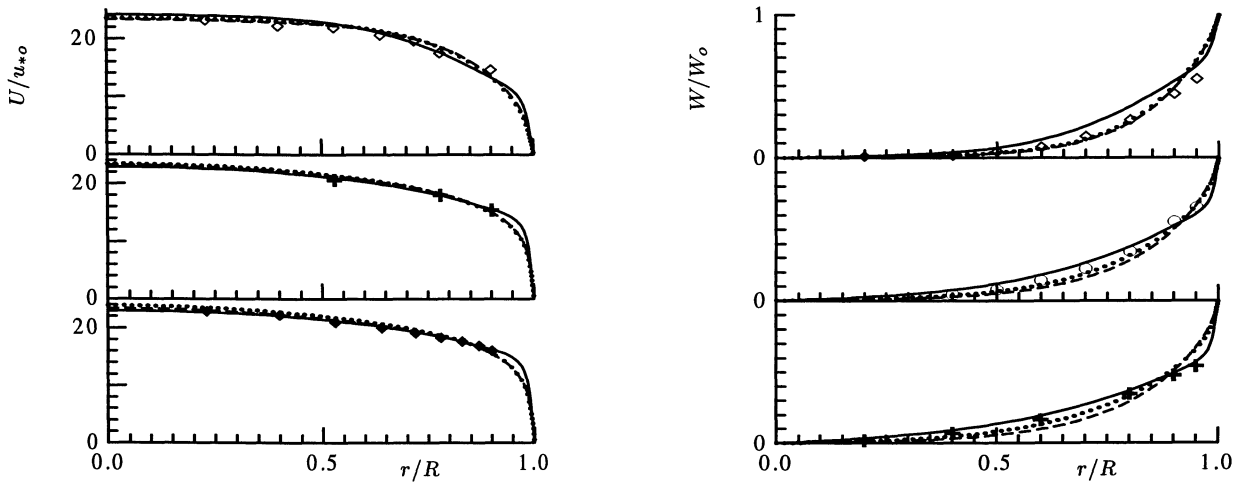


Figure 3: Mean velocity components. Calculations:( —— ) Q2, (--- ) IP, (····· ) SSG1;
experiments (Zaets et al., 1985): (♦) $N = 0.$, (+) $N = 0.15$, (o) $N = 0.3$, (◊) $N = 0.6$

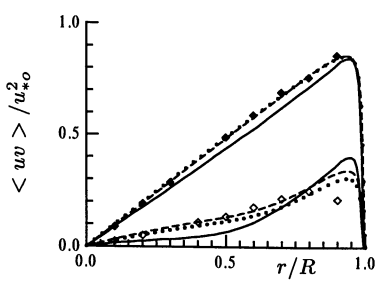


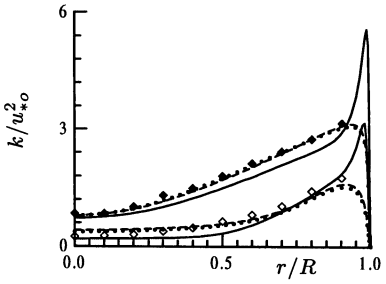


Figure 4: (see denotations on Figure 3)

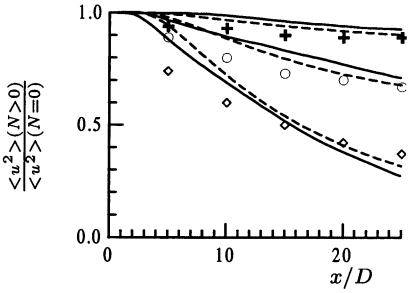


Figure 5: $r/R = 0.6$

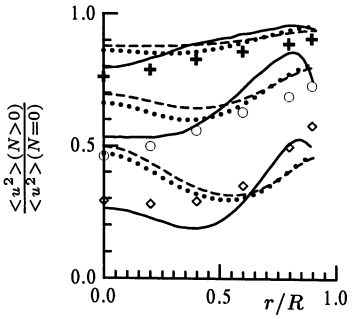


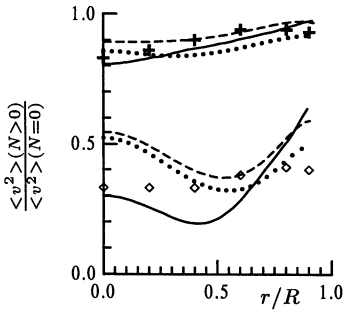


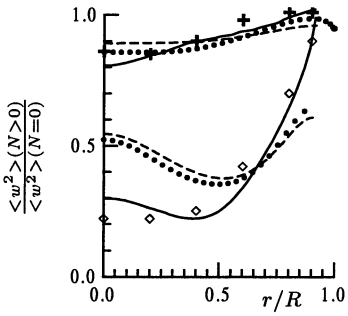


Figure 6: (see denotations on Figure 3)

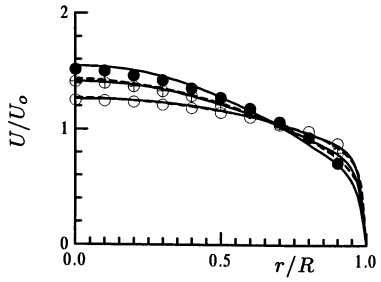


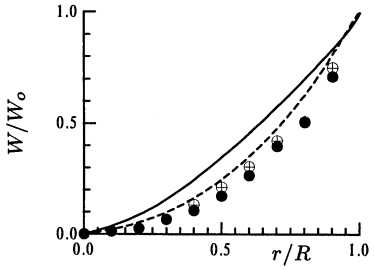


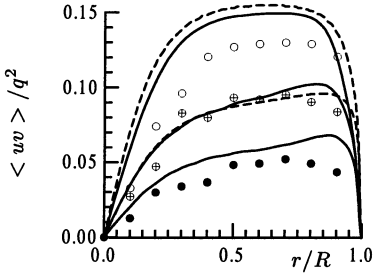


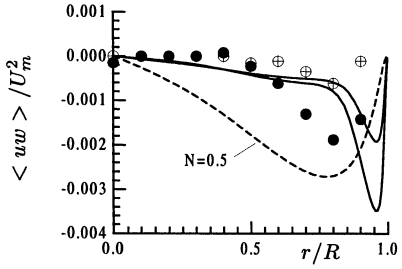


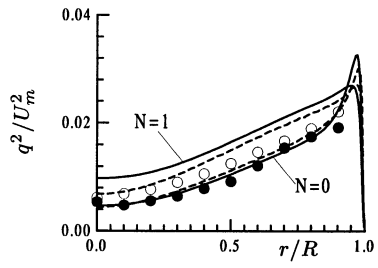


Figure 7: Fully developed pipe flow ($Re_o = 2 \cdot 10^4$). Calculations:( —— ) Q1, (--- ) SSG2; experiments (Imao et al., 1996): (○) $N = 0.$, (⊕) $N = 0.5$, (●) $N = 1.$